ISBN: 978-3-95450-232-5 ISSN: 2673-7000 doi:10.18429/JACoW-NAPAC2022-MOPA02

ACTIVATION OF THE IBA PROTEUS ONE PROTON THERAPY BEAMLINE USING BDSIM AND FISPACT-II

E. Ramoisiaux, C. Hernalsteens[1], R. Tesse, E. Gnacadja, N. Pauly, M. Vanwelde
Service de Métrologie Nucléaire, Université libre de Bruxelles, Brussels, Belgium
[1]also at CERN, Geneva, Switzerland

Abstract

Cyclotron-based proton therapy systems generate large fluxes of secondary particles due to the beam interactions with the beamline elements, with the energy degrader being the dominant source. Compact systems exacerbate these challenges for concrete shielding and beamline element activation. Our implementation of the Rigorous Two-Step method uses Beam Delivery Simulation (BDSIM), a Geant4-based particle tracking code, for primary and secondary particles transport and fluence scoring, and FISPACT-II for time-dependent nuclear inventory and solving the rate equations. This approach is applied to the Ion Beam Applications (IBA) Proteus®ONE (P1) system, for which a complete model has been built, validated, and used for shielding activation simulations. We detail the first simulations of the activation on quadrupole magnets in high-fluence locations downstream of the degrader. Results show the evolution of the long-lived nuclide concentrations for short and long timescales throughout the facility lifetime for a typical operation scenario.

INTRODUCTION

Cyclotron-based proton therapy systems require an energy degradation system to deliver proton beams from 230 MeV to any desired energy down to 70 MeV covering treatments energy requirements. The interaction of the primary beam with the degrader scatters the primary protons and produces a large number of secondary particles, mainly neutrons [1]. The lost protons and secondary neutrons interact with the beamline elements or the concrete shielding via nuclear reactions, mainly capture and spallation, producing radioactive nuclides; some are long-lived and are responsible for the long-term activation of the proton therapy system and its concrete shielding.

While next-generation proton therapy systems evolve towards more compact designs, research activities requiring higher currents and extended irradiation periods are often conducted in parallel with patient treatments. Consequently, close activation monitoring of the beamline and shielding is a requirement when designing new compact treatment centres.

To tackle this challenge, we established the BDSIM/FISPACT-II methodology, inspired by the Rigorous Two-Step (R2S) method [2], coupling Beam Delivery SIMulation (BDSIM) [3], a Geant4-based particle tracking code, with the code and library database FISPACT-II [4]. This methodology, thoroughly detailed in Ref. [5, 6], was applied to the shielding design of the future proton therapy centre of Charleroi, Belgium. The BDSIM model of the IBA Proteus®ONE proton therapy system was already developed and validated against experimental data [7].

We use the BDSIM/FISPACT-II methodology to characterise the activation of critical beamline elements in high fluence regions during a typical centre lifespan of 20 years and help prepare the future centre decommissioning. This method will be applied on the first quadrupole of the rotating gantry, called Q1G, which was modelled using a cylindrical default geometry made of iron provided by BDSIM. Q1G is placed downstream from the degrader in the shielding wall connecting the vault to the treatment room. Q1G was chosen for this study as its location in the beamline implies that it is exposed to the secondary particles fluence generated from the beam interaction with all the extraction line elements. Figure 1 shows the BDSIM model of the vault with the superconducting synchro-cyclotron (S2C2), the extraction line with the quadrupoles, slits and degrader, and the start of the rotating gantry with the collimator and Q1G. The complex geometries of the S2C2, the degrader, the collimator and the concrete shielding have been implemented in the BDSIM model using Geometry Description Markup Language (GDML) files created for Geant4 by the Python library PYG4OMETRY [8, 9].

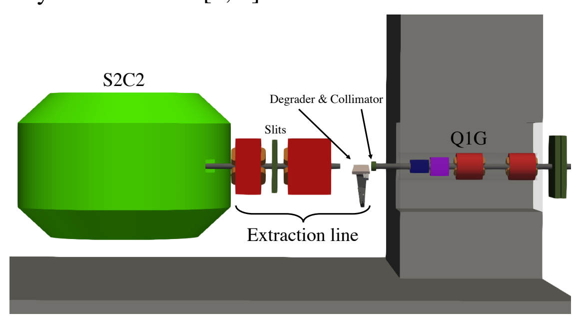

Figure 1: BDSIM model of the vault extraction line and its shielding. The S2C2 and the energy degradation system are shown. The concrete shielding wall separating the cyclotron vault from the treatment area is visible, with the beamline elements fit through a cylindrical cut.

The activity of a compound is determined by its clearance index. The clearance index is defined as the sum A_i/CL_i over all the material radionuclides with A the specific activity and CL the clearance level allowed by the Belgian legislation. If the clearance index exceeds the value of 1, the compound is considered radioactive waste. The main isotopes produced in concrete are listed in Table 1 with their corresponding clearance level.

Table 1: Clearance levels for the main isotopes produced in iron. Data taken from FISPACT-II database.

Nuclide	CL (Bq/g)	Nuclide	CL (Bq/g)
^{54}Mn	0.1	^{49}V	770
^{55}Fe	1000	^{44}Ti	7.2
^{3}H	100	^{57}Co	1

ISBN: 978-3-95450-232-5 ISSN: 2673-7000 doi:10.18429/JACoW-NAPAC2022-MOPA02

TOOLS AND METHODS

Primary beam tracking simulations from the exit of the S2C2 to the isocenter have been realised using the BDSIM model with the degrader calibrated for a delivered beam energy of 100 MeV, which is the future centre most-used value. The irradiation condition studied are those used during the centre dimensioning [5]: 300 hours of irradiations per year with an S2C2 current of 150 nA.

The differential fluence of the secondary neutrons and lost protons are scored following respectively the predefined energy group structures "CCFE-709" and "CCFE-162" in the cylindrical scorer mesh presented in Fig. 2 using the 4D-Scoring BDSIM feature [10]. The scorer mesh has been defined with 5 bins along the radius and 20 bins along the length so the last radial bin encompasses the iron quadrupole structure.

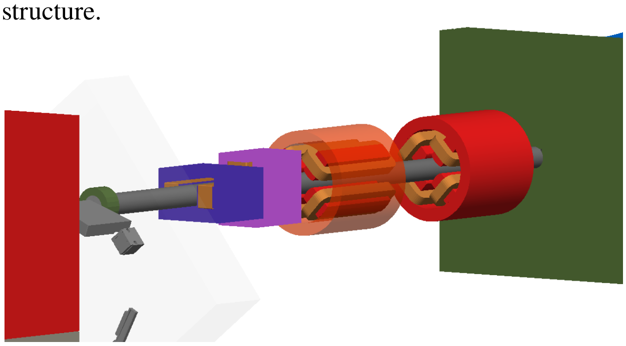

Figure 2: Detailed model of the energy degrader and the beginning of the rotating gantry. A cylindrical 4D-Scoring is placed on the Q1G quadrupole. The last radial bin fits the iron external geometry of the magnet. On the figure, the external geometry of Q1G was removed and the last bin of the scoring mesh was highlighted in red.

The neutron and proton differential fluence is presented on Fig. 3 at different depths. One can observe that the neutron fluence variation with depth is less important than the proton fluence variation. This is expected behaviour due to the finite range of protons in iron. The level scheme observed in the neutron and proton differential fluences can be directly linked to the variation in energy bin widths of their respective energy group structure.

The differential fluences are then provided to FISPACT-II to compute the activation of Q1G over an irradiation and a cooling period of 20 years separately for each type of particle. The results are then combined to characterise the total activation of Q1G at the end of the centre lifespan. Figure 4 compares the clearance level along Q1G length induced by either the neutrons or the protons interactions with iron. One can observe that neutron activation dominates at all depths with only a small impact of the proton activation in the first centimetres. On the other hand, the high clearance index value shows that the quadrupole structure will be highly activated at the decommissioning time of the centre.

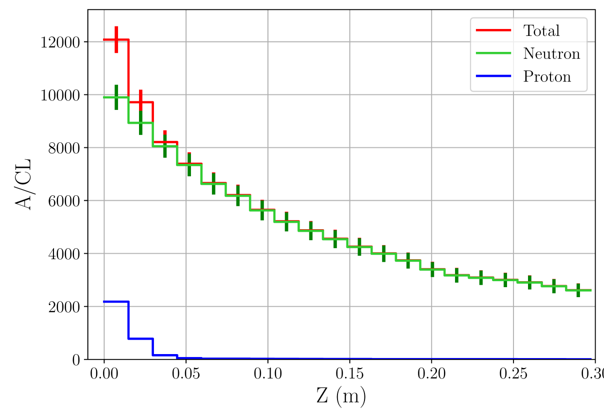

Figure 4: Evolution of the clearance index along with the thickness of the Q1G external structure. The clearance indexes related to the neutron and proton activation are represented in green and blue, while the total is represented in red.

FISPACT-II allows to study the evolution in time of the activation and gives separately the impact of each radioactive nuclide. Figure 5 shows the evolution of the clearance index of the most radioactive part of the Q1G structure during the irradiation and the cooling periods. An equilibrium is reached after 7 years in the facility lifetime. On the other

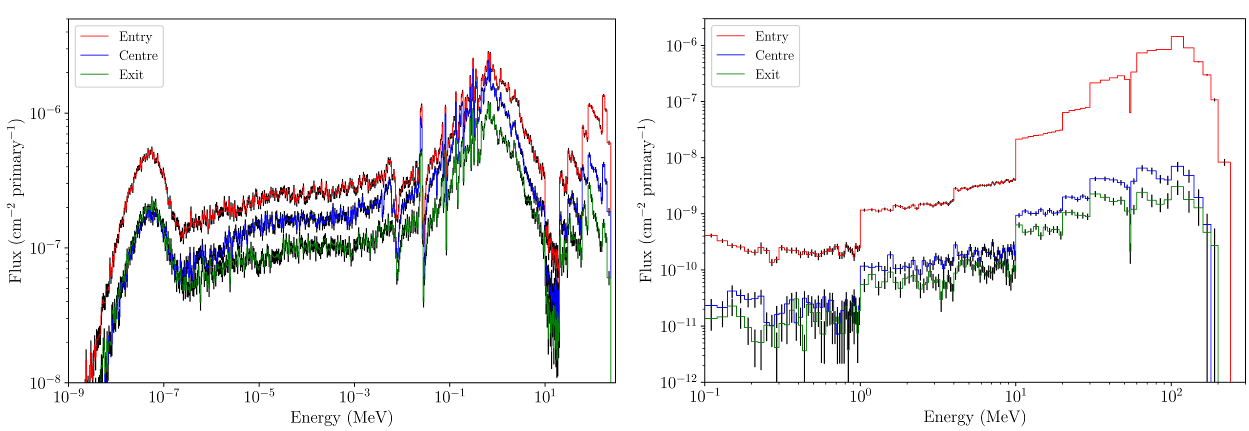

Figure 3: Differential secondary neutron fluence (left) and proton fluence (right) extracted from the Q1G external structure using the BDSIM 4D Scoring feature. The fluence has been extracted at the entry, the centre and the exit of the Q1G outer structure. The energy bins follow the CCFE-709 and CCFE-162 energy group structures, respectively.

ISBN: 978-3-95450-232-5 ISSN: 2673-7000 doi:10.18429/JACoW-NAPAC2022-MOPA02

hand, a cooling period of 15 years is required for the external structure of Q1G to be totally considered as normal waste.

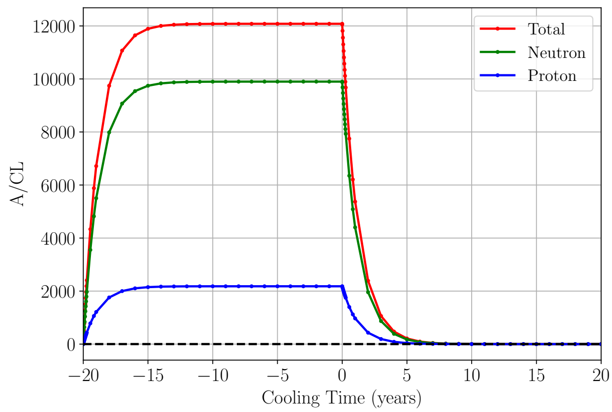

Figure 5: Evolution of the clearance index with time of the most radioactive part of the Q1G external structure following the incident particle type.

The results show that the radioactivity is mainly induced by one radioactive nuclide, ^{54}Mn. The activity evolution of the other radioactive nuclides was also studied. Figure 6 presents the evolution of the clearance index induced by the radioactive nuclides, other than ^{54}Mn. Such accurate knowledge of the radioactive nuclides concentration in the iron during the centre lifetime can be useful for radioprotection studies and activity measurement campaign designs.

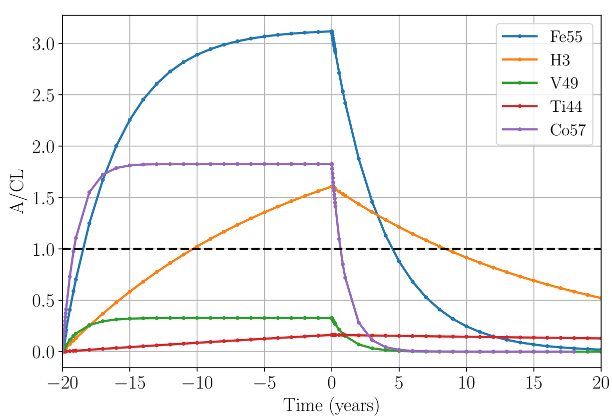

Figure 6: Evolution of the clearance index with time of the most radioactive part of the Q1G external structure following the main radioactive nuclides, other than ^{54}Mn.

This activation study can be extrapolated to the other critical elements of the beamline or the movable parts which are brought in the vault or the treatment room for specific treatment plans as eye treatment nozzle or for research activities as an additional energy degradation system, electronic systems and materials for the spatial industry or biological tissue sampler holders.

CONCLUSION AND OUTLOOKS

The BDSIM/FISPACT-II methodology has been applied to the specific case of the activation of an element of the P1 beamline. The first quadrupole of the rotating gantry, Q1G, has been chosen as its position behind the degrader leads to significant irradiation of scattered protons and secondary neutrons. The differential fluence scoring has been realised using a cylindrical 4D scorer mesh whose last radial bin encompasses the iron external structure of the magnet and whose energy binning follows the required energy group structure for both incident particles. The results showed that the neutron-induced activation dominated the proton-induced activation. The analysis of the radioactive nuclide concentrations evolution with time showed that ^{54}Mn was the primary source of activity and that a cooling period of 15 years after the centre decommissioning will be required for the Q1G structure to be considered as normal waste.

The BDSIM/FISPACT-II methodology will be used for a complete activation study of all the P1 beamline elements and experimental setup structures of the future proton therapy centre of Charleroi.

ACKNOWLEDGMENT

This work has received funding from the Walloon Region (SPW-EER) Win^{2}Wal program under grant agreement No. 1810110 and PIT Prother-wal program under grant agreement No. 7289. The authors thank IBA for the support provided during this work.

REFERENCES

[1] H. Paganetti, *Proton Therapy Physics*. CRC Press, MGH and HMS, Boston, USA, 2011.

[2] Y. Chen and U. Fischer, "Rigorous mcnp based shutdown dose rate calculations: Computational scheme, verification calculations and application to ITER," *Fusion Eng. Des.*, vol. 63-64, pp. 107–114, 2002. doi:10.1016/S0920-3796(02)00144-8

[3] L. J. Nevay *et al.*, "BDSIM: An accelerator tracking code with particle-matter interactions," *Comput. Phys. Commun*, vol. 252, p. 107 200, 2020. doi:10.48550/arXiv.1808.10745

[4] J.-C. Sublet *et al.*, "FISPACT-II: An advanced simulation system for activation, transmutation and material modelling," *Nucl. Data Sheets*, vol. 139, pp. 77–137, 2017. doi:10.1016/j.nds.2017.01.002

[5] E. Ramoisiaux *et al.*, "Self-consistent numerical evaluation of concrete shielding activation for proton therapy systems," *Eur. Phys. J. Plus*, vol. 137, p. 889, 2022. doi:10.1140/epjp/s13360-022-02960-9

[6] E. Ramoisiaux *et al.*, "Concrete Shielding Activation for Proton Therapy Systems Using BDSIM and FISPACT-II," in *Proc. IPAC'22*, Bangkok, Thailand, 2022, p. 728. doi:10.18429/JACoW-IPAC2022-MOPOMS041

[7] C. Hernalsteens *et al.*, "A novel approach to seamless simulations of compact hadron therapy systems for self-consistent evaluation of dosimetric and radiation protection quantities," *EPL*, vol. 132, p. 50 004, 2021. doi:10.1209/0295-5075/132/50004

[8] S. Boogert *et al.*, "Pyg4ometry : A tool to create geometries for Geant4, BDSIM, G4Beamline and FLUKA for particle loss and energy deposit studies," in *IPAC2019, Melbourne, Australia*, 2019. doi:10.18429/JACoW-IPAC2019-WEPTS054

ISBN: 978-3-95450-232-5 ISSN: 2673-7000 doi:10.18429/JACoW-NAPAC2022-MOPA02

[9] S. Walker *et al.*, “Pyg4ometry: A python library for the creation of monte carlo radiation transport physical geometries,” *Comput. Phys. Commun*, vol. 272, p. 108 228, 2022. doi:10.1016/j.cpc.2021.108228

[10] E. Ramoisiaux *et al.*, “BDSIM Developments for Hadron Therapy Centre Applications,” in *Proc. IPAC’21*, Campinas, Brazil, May 2021, pp. 1252–1255. doi:10.18429/JACoW-IPAC2021-MOPAB416